Hue University Journal of Science: Natural Science
Vol. 134, No. 1S-1, 127–140, 2025 (Special Issue: IFGTM 2025)

pISSN 1859-1388
eISSN 2615-9678

Analysis of Riverine Flood Dynamics by using Sentinel-1 Satellite Imagery in An Giang, Vietnam

Ho Ngoc Nhu Y[1], Sameh A. Kantoush[2], Manh-Hung Le[3, 4], Duong Cao Phan[5], Doan Van Binh[1]*

[1] Faculty of Engineering, Vietnamese-German University, Ho Chi Minh City, Vietnam
[2] Disaster Prevention Research Institute, Kyoto University, Goka-sho, Uji City, Kyoto, Japan
[3] Hydrological Sciences Laboratory, NASA Goddard Space Flight Center, Greenbelt, MD, USA
[4] Science Applications International Corporation, Greenbelt, MD, USA
[5] Ireland's Centre for AI, School of Computer Science, University of Dublin, Belfield, Dublin 4, Ireland

* Correspondence to Doan Van Binh <binh.dv@vgu.edu.vn>

(*Received: 23 June 2025; Revised: 19 December 2025; Accepted: 19 December 2025*)

Abstract. The Vietnamese Mekong Delta (VMD) is frequently affected by seasonal floods, especially with An Giang Province being one of the most vulnerable regions. In the context of climate change and human activities, such as dam construction and dyke development, the flood regime in this area is rapidly and unpredictably changing. These alterations have exacerbated challenges in agriculture, water management, and local livelihoods, yet reliable long-term flood maps and early-warning tools remain limited. This study used Sentinel-1 satellite imagery on the Google Earth Engine (GEE) platform to monitor and evaluate flood dynamics in An Giang from 2015 to 2024. The results show that flooding still occurred in low-lying areas without closed-dike protection, though the overall flooded extent slightly decreased during 2015–2024. However, the annual patterns showed considerable variability: while 2017–2018 recorded extensive flooding with peak inundation exceeding 30,000 ha, 2019–2020 experienced minimal flood extent. This sharp contrast highlights the increasing irregularity of the flood regime in An Giang. This study created a long-term remote sensing dataset for An Giang by using Sentinel-1 and GEE, providing a scientific basis for flood monitoring, agricultural adaptation, and advancing remote sensing applications in deltaic flood monitoring.

Keywords: Vietnamese Mekong Delta, flooding, remote sensing, Sentinel-1

1 Introduction

The Vietnamese Mekong Delta (VMD) is the largest in Vietnam and ranks third globally in terms of area, covering approximately 40,000 km². This region is Vietnam's most important agricultural production centre, contributing nearly 50% of the country's total rice production, 60% of aquaculture output, and over 70% of fruit production. Notably, over 90% of Vietnam's rice exports originate from the VMD [1], highlighting its pivotal role in regional food security and the country's agricultural export economy.

An Giang Province is one of the most prominent provinces in the VMD, located in the upstream region and bordering Cambodia. With an area of approximately 3,537 km² and a population exceeding 2.4 million people, An Giang is the most densely populated province in the region [2]. The province features a complex hydrological system, encompassing both main branches of the Mekong River: the Tien River and the Hau River. This strategic location regularly subjects An Giang to seasonal flooding from upstream areas, solidifying its role as a significant agricultural production centre. The province produces approximately 3.9 million tons of rice annually and ranks first nationally in per capita rice production [3]. Historically, the low-lying topography of An Giang has facilitated seasonal flooding, which provides numerous

benefits, including sediment deposition and natural fishery resources, thereby supporting both agricultural and aquaculture production. The province also functions as a central flood retention area, alleviating flood pressure on downstream provinces. However, these characteristics also make An Giang one of the most vulnerable areas to hydrological and climatic variations. As an upstream province, An Giang faces more severe flood impacts than downstream provinces. Before the construction of closed-dike systems, 60–70% of the province's agricultural land was flooded annually (with depths of 1–2.5 m), leading to significant crop losses and disruptions to transportation, infrastructure, schools, and local livelihoods [4].

In recent decades, flood cycles and intensities in the VMD have undergone significant changes, with An Giang experiencing notable shifts in flood frequency, timing, and depth [5]. One primary factor contributing to this is the development of hydroelectric dams in the upper Mekong River basin. As of 2020, more than 13 large hydroelectric dams have been constructed along the Mekong River's mainstem, primarily in China and Laos [6, 7]. These dams regulate water flow, significantly reducing the volume of water reaching the VMD during the rainy season while increasing flow during the dry season, thereby disrupting the natural hydrological patterns of the VMD [8]. Additionally, the flood control infrastructure, including the closed-dike system in An Giang designed to support three consecutive rice crops, has led to substantial changes in the region's flood regimes. Since 2000, nearly 329 km of dikes have been constructed to retain internal water and prevent external water intrusion, aiming to increase production cycles and protect residents' property [4]. However, this dike system has reduced natural floodplain areas and diminished flood storage capacity, thereby altering flood propagation patterns across the region [9]. Climate change has further exacerbated flood impacts in the VMD. Shifts in the rainfall distribution patterns indicate a decrease in the number of rainy days, whereas the frequency and intensity of extreme rainfall events have increased. This trend is especially pronounced during the rainy season, with more days recording rainfall exceeding 10 mm and 20 mm [10]. These changes affect agricultural production and the ecological services provided by flooding, such as reducing salinity intrusion in the downstream region, regenerating fishery resources, and restoring groundwater balance.

Continuous flood monitoring and surveillance are essential in the context of increasingly complex and unpredictable flood patterns, resulting from climate change and human activities. Traditional methods, which rely on data from observation stations, are often limited in spatial coverage, lack real-time updates, and struggle to respond promptly to large-scale flood events [11]. Therefore, remote sensing technology is becoming increasingly utilised for flood monitoring because of its ability to provide remote observations, broad regional coverage, continuous data collection, and cost-effectiveness. Synthetic Aperture Radar (SAR) sensors from Sentinel-1 satellites, developed by the European Space Agency (ESA), can collect data through clouds and fog, and can operate both day and night. This makes them particularly useful during flood seasons in the VMD, when persistent cloud cover and rainy weather conditions are common [12]. With short revisit intervals (every 6 days), high resolution, and free access via the Google Earth Engine, Sentinel-1 data facilitates efficient data collection, integration, and automated processing workflows [11]. When combined with automatic thresholding algorithms such as the Otsu algorithm, Sentinel-1 imagery can effectively distinguish between flooded and non-flooded areas, particularly flat areas like An Giang [13].

Recent advances in remote sensing technology have made large-scale monitoring of surface water and flood feasible and effective. Various satellite products, including Landsat, Sentinel-1, Sentinel-2, and MODIS, can be used for flood monitoring. In the early stages, studies primarily relied on MODIS data, particularly MODIS time series, to monitor changes in annual flood extent in the VMD over five flood seasons (2000–2004) [14]. These studies also analysed flood dynamics in the

pISSN 1859-1388
eISSN 2615-9678

VMD over a more extended period (2000–2013) and assessed the impacts of hydraulic works on flood regimes [15]. Additionally, Sentinel-1 SAR data have also been extensively applied in numerous studies for flood detection, benefiting from its ability to observe through clouds and its frequent revisit time of every 6 days. At the global scale, several studies have demonstrated that Sentinel-1 time series can effectively track inundation, even in temporarily flooded vegetation, thereby enhancing flood detection over time [16]. In disaster response, the Otsu thresholding method, implemented on GEE, has been effectively used to produce rapid flood maps for major flood events such as the 2018 Kerala flood [17]. More recently, Misra et al. [18] applied a deep learning model to ten years of Sentinel-1 data to create a global flood map, analysing vulnerable regions such as Ethiopia and Kenya during 2014–2024. In Bangladesh, Uddin et al. [19] developed an operational workflow for rapid flood mapping in 2017, achieving an overall accuracy of 96.4% by combining Sentinel-1 with land cover information from Landsat-8.

In Vietnam, Sentinel-1 has been increasingly applied to different purposes. In the VMD, Lam et al. [20] utilised a Sentinel-1 time series combined with machine learning models (CNN, MLP, RF) to classify flood and flood-prone areas, highlighting the potential of SAR data for large delta regions. In central Vietnam, a study in Hoa Vang (Da Nang) mapped the peak flood extent in 2022 on the GEE platform and assessed its impact on agricultural land [21]. In the lower Con River basin, a thresholding approach using VV backscatter values (−23 to −12 dB) was applied to 28 Sentinel-1A scenes to detect rapid flood dynamics [22]. For urban areas, a flood risk assessment framework utilising Sentinel-1 on GEE was developed for Thai Nguyen City [23]. In addition, a study on Tropical Storm Talas (2017) demonstrated that Sentinel-1, combined with the Otsu method, can effectively map flood extent and estimate rice damage under extreme weather conditions [24]. In An Giang, Tran et al. [13] applied a Sentinel-1 time series combined with dynamic Otsu thresholding to map surface water, achieving high accuracy (R^2 = 0.97 for rivers; R^2 = 0.88 in paddy fields; RMSE ~1–4%). Nguyen et al. [25] employed Sentinel-1A to map inundation depth across the province, while Afifi and Magdy [26] utilised the Global Flood Mapper on GEE with Sentinel-1 data to enable rapid flood monitoring in the region.

Although these studies confirm the effectiveness of Sentinel-1 for flood monitoring, especially in tropical climate regions and often in cloudy areas, such as the VMD, most of them are event-based or localised, and have yet to provide a long-term, multi-year assessment. To address these gaps, this study utilises Sentinel-1 Synthetic Aperture Radar, developed by the European Space Agency, which can collect data through clouds and fog, operating day and night. This capability is particularly useful under cloudy and prolonged rainy weather conditions during flood seasons in the VMD [12] with short revisit time (6 days), spatial resolution of 20 × 22 m, and pixel spacing of 10 × 10 m [27]. The free availability of Sentinel-1 data on the Google Earth Engine facilitates easy collection, integration, and automated processing workflows [11]. When combined with automatic thresholding algorithms, such as the Otsu algorithm, Sentinel-1 imagery accurately differentiates between flooded and non-flooded areas, particularly in flat areas as seen in An Giang [13].

With the above-mentioned capacities, the continuous data collection process is ensured throughout the 6-month rainy season. In the context of declining floods and their impacts on socio-economic activities in An Giang, this study aims to achieve two primary objectives: (1) identify trends in flood extent changes and (2) analyse the spatio-temporal dynamics of flooding in An Giang Province.

2 Study area

An Giang Province is situated in the upper part of the VMD in southern Vietnam (Fig. 1). The province shares a border with Cambodia to the northwest, marked by a boundary line that extends over 100 kilometres. It borders Dong Thap Province to the east, Can Tho to the

southeast, and Kien Giang to the southwest [28]. With a total area of approximately 3,537 km², An Giang accounts for nearly 9% of the total area of the VMD region [29]. The province is the most densely populated area in the VMD and ranks eighth nationally, with over 2.4 million inhabitants [30]. An Giang plays a crucial role in the hydrological structure and flood regulation of the entire downstream VMD area, acting as the main entry point for floods from the upstream Mekong River through Cambodia and as a flood retention region for downstream provinces [31]. This strategic position makes it the most significantly affected by changes in the flood regime of the Mekong River. The province has also implemented flood control measures with great strength, including building dike systems and modifying farming models to adapt to changing flood patterns.

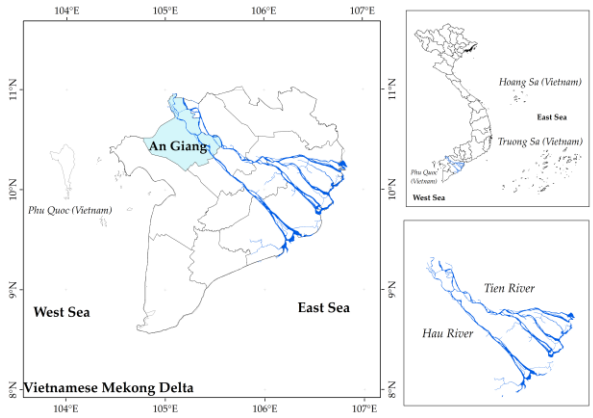

Fig. 1. Location of An Giang Province

The VMD region, including An Giang Province, has a tropical monsoon climate near the equator with two distinct seasons: the dry season (December–April) and the rainy season (May–November) [32]. The average annual rainfall ranges from 1,400 to 2,400 mm, with the majority falling during the rainy season, accounting for more than 90% of the total annual precipitation [33, 34]. Owing to its low-lying deltaic terrain (with an average elevation ranging from 0.5 to 2 m), An Giang is prone to flooding, particularly during peak flood months from September to November. The terrain slopes gently from north to south and southeast to west, creating favourable conditions for flood flows from the upstream Mekong River [35]. An Giang's river and canal system is exceptionally dense, serving as a water source for daily life, agricultural production, and a natural flood drainage channel. Owing to its low terrain characteristics, dense hydrological system, and concentrated rainfall during the flood season, An Giang has become one of the most flood-affected localities in the VMD region.

The flood season in An Giang typically begins in July, with peak floods usually occurring from September to November, with an average flood depth ranging from 0.5 to 2.5 m, depending on the terrain and regional irrigation system. However, in recent years, reflecting the combined impact of upstream hydroelectric projects and flood-control infrastructure, floods in An Giang have tended to arrive later, with lower water levels and shorter inundation periods [36]. These alterations have reduced the role of natural flood regulation while simultaneously affecting agricultural production and local aquatic resources.

The development of the dike system in An Giang was primarily aimed at flood control and facilitating the transition from a double rice crop model to a triple rice crop model, increasing the area under this model from less than 20% in 2000 to 80% in 2018 [37], thus increasing rice production. However, this triple rice crop model has several negative consequences, including reduced natural flood storage capacity, soil degradation due to annual sediment loss, and a decline in biodiversity, particularly the loss of natural aquatic resources associated with the flood season [38]. These changes in the hydrological system, flood control system, and cropping seasons require widespread monitoring that is both up-to-date and objective.

pISSN 1859-1388
eISSN 2615-9678

3 Materials and methods

3.1 Materials

This study used the Sentinel-1 satellite image dataset, which was collected directly from the GEE platform. The Sentinel-1 satellite images belong to the Ground Range Detected (GRD) dataset provided by the ESA. Sentinel-1 is a synthetic aperture radar satellite system that uses the C band, allowing image acquisition in all weather and lighting conditions. This feature is especially suitable for areas with tropical weather conditions, such as the VMD, where the rainy season lasts for six consecutive months.

The Sentinel-1 GRD satellite image data is corrected for terrain and radiation. The satellite scan mode is Interferometric Wide Swath (IW), with a pixel spacing of 10 × 10 m and a ground resolution of 20 × 22 m, and a revisit period of six days [27]**.** In this study, we used the VH (Vertical transmit – Horizontal receive) polarisation channel, which is highly sensitive to water and effective for flood detection than the VV polarisation channel in lowland agriculture areas [13]. The data we collected spanned from 2015 to 2024, encompassing both the dry and rainy seasons.

Sentinel-1 satellite images collected from GEE library have already undergone basic preprocessing steps, including thermal noise removal, radiometric calibration to convert data into backscatter coefficients (sigma nought, dB unit), and terrain correction via the SRTM digital elevation model [39]. Additional processing steps specific to this study are described in the methodology section. Owing to the large data size and processing limitations of GEE, we divided the entire area into district-level administrative units for processing and analysis. In this regard, Sentinel-1 data were processed independently for each district, generating monthly flood maps from 2015 to 2024. After processing, the flood maps were downloaded and merged by using ArcGIS software to create a composite map showing the extent of flooding across the entire An Giang Province.

3.2 Methodology

This study follows a series of steps for detecting and analysing floods, as shown in Fig. 2: (i) defining the study area and collecting Sentinel-1 satellite data, (ii) preprocessing the radar images, (iii) reducing speckle noise via the Refined Lee filter, (iv) applying the dynamic Otsu thresholding method to separate flooded and non-flooded areas, (v) creating flood maps by comparing dry and flood season images, and (vi) calculating the flooded areas. These steps were implemented on the GEE platform.

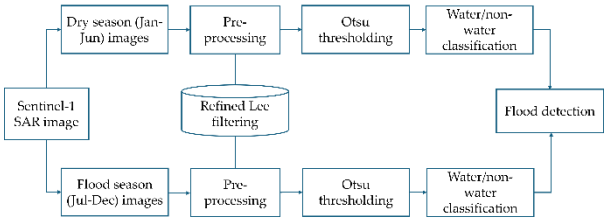

Fig. 2. Flood detection via the Sentinel-1 workflow

Step 1: Collecting Sentinel-1 satellite image data. The study area is An Giang Province, chosen for its frequent seasonal flooding and clear evidence of flood reduction. Sentinel-1 GRD radar imagery was retrieved from the COPERNICUS/S1-GRD data catalogue. The images were filtered according to date to represent the dry season (January–May) and the flood season (June–December) from 2015 to 2024. Only VH polarisation images were used.

Step 2: Image preprocessing. The Sentinel-1 GRD images from the GEE were preprocessed by ESA, which included edge noise removal, radiometric calibration, and terrain correction [39]. In addition, to filter speckle noise, the VH images were converted from decibels (dB) to a natural scale (σ_{Linear}) according to formula (1).

$$\sigma_{Linear} = 10^{\left(\frac{\sigma^0_{dB}}{10}\right)} \quad (1)$$

Filtering speckle noise via the refined Lee filter: SAR data is often affected by speckle noise [40]. To address this, the Refine Lee filter was applied, which uses multiple gradient-oriented kernels and calculates the local variance to adjust the smoothing coefficient. This approach helps reduce noise while preserving edge details [41].

Step 3: Dynamic Otsu thresholding. After filtering noise, each Sentinel-1 image from the acquisition dates was classified into water and non-water classes by using the dynamic Otsu thresholding algorithm. The Otsu threshold determines an optimal threshold value t by analysing the image histogram and minimising the intra-class variance between two categories (water and non-water) [13]. The algorithm is applied according to formula (2)

$$\sigma^2(t) = P_\omega(t).\sigma^2_\omega(t) + P_{n\omega}(t).\sigma^2_{n\omega}(t) \quad (2)$$

where t is the optimal threshold; P_ω and $P_{n\omega}$ are the water and non-water class probabilities, respectively; σ^2_ω, and $\sigma^2_{n\omega}$ are the respective variances of each class. With threshold t, the flooded area is defined as pixels with values greater than the threshold in the dry season and less than the threshold in the rainy season.

Step 4: Flood detection. Flood detection was performed by comparing the water/non-water classification results between the dry and flood seasons. This step aims to distinguish permanent water bodies (e.g., rivers and lakes) from seasonally flooded areas that appear only during the flood season. A pixel was classified as flooded if the backscatter value was higher than the threshold in the dry season (non-water) but dropped below the threshold in the flood season (water). A pixel was classified as non-flooded if it remained above the threshold in both the dry and flood seasons.

Step 5: Calculating the flooded area. The flooded areas were represented as binary masks. Each flood mask was multiplied by the pixel area layer to estimate the flood extent in square meters, which was then converted to hectares.

The Otsu thresholding algorithm was employed to automatically separate water and non-water classes from the Sentinel-1 VH backscatter histograms. The method is fully automatic, as the optimal threshold is computed by minimising the within-class variance of two distributions without requiring any user-defined parameters. Nevertheless, the final threshold value is indirectly influenced by several choices in the processing pipeline. Specifically, the histogram depends on the input image composites (dry- and flood-season means), the spatial extent over which the histogram is calculated (here, the entire An Giang Province), the spatial resolution of analysis (30 m), and the application of speckle filtering (Refined Lee). Although Otsu itself is parameter-free, the selection of input data and pre-processing settings function as hyperparameters, which can affect the final threshold outcome.

4 Results

4.1 Spatial distribution of seasonal flooding in An Giang

Fig. 3 illustrates the seasonal variations in flood extent in An Giang Province, showing the timing of when the flood starts, peaks, and recedes by considering the mean monthly values from 2015 to 2024. For instance, in July, flooding began to occur in relatively low-flooded areas (flooded areas constitute more than 3% of the study area). The flooded area increased rapidly in August and September, reaching approximately 10% and 15% of the area of An Giang, respectively. October marked the peak flood period, with the highest average flooded area exceeding 24% of the total area. During November–December, floods began

pISSN 1859-1388
eISSN 2615-9678

to recede but remained at high levels (20% and 16% of the study area were flooded), demonstrating prolonged water retention capacity in low-lying areas.

During the early flood months (July and August), the flooded area remained limited and scattered, mainly concentrated in low-lying areas near borders, such as the An Phu, Tinh Bien, and Tri Ton districts. These areas have low topography and are near border gates, typically experiencing early impacts from the upstream flood wave from the Mekong River and the overflow from the Cambodian floodplains. During the flood peak period (September to November), the flooded area expanded significantly, particularly in the central and western parts of the province, including Chau Phu, Thoai Son, and Tri Ton. In contrast, areas such as Cho Moi, Long Xuyen, and parts of Chau Thanh, which are protected by closed-dike systems, had minimal flooding on the maps. This intra-seasonal analysis demonstrates that flood peaks were temporally concentrated in October, while both topographic conditions and the presence of dike systems strongly influenced spatial inundation patterns.

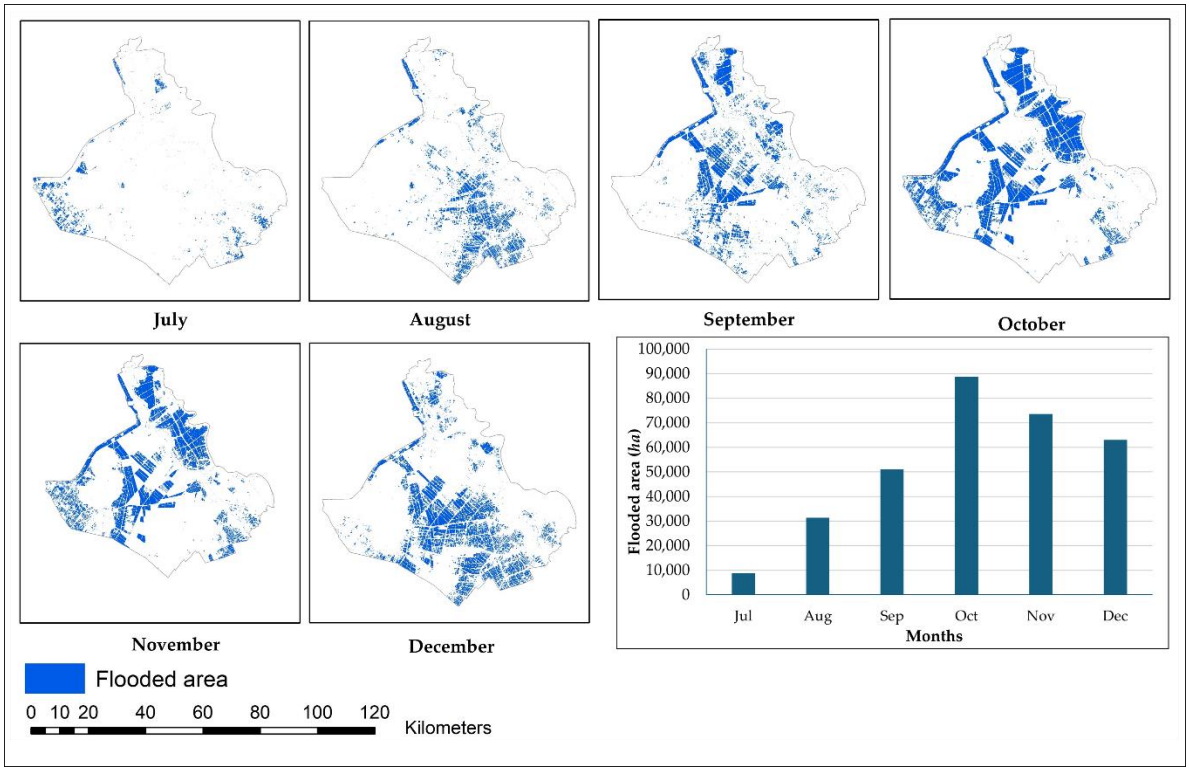

Fig. 3. Monthly spatial distribution and flood extent in An Giang Province during rainy season (July–December), averaged from 2015 to 2024

4.2 Monthly flood dynamics from 2015 to 2024

The heatmap displaying monthly flood area variations in An Giang Province from 2015 to 2024 (Fig. 4) reveals significant fluctuations in flood timing, intensity, and annual trends. Years such as 2018 and 2022 recorded the largest flooded areas in the series, with peak values reaching 31% of the province's area in September 2018 and 28% in October 2022. These indicate that major floods can still occur in An Giang, despite the general decline in floods in the VMD. In contrast, 2020 and 2021 had minimal flooding, with flooded areas accounting for only 8% of the total area in September 2021 and 16% in October 2020.

Flood arrival and recession timing also altered significantly (Fig. 3). In some years (e.g., 2017 and 2018), floods arrived early, with extensive inundation beginning as early as August (14% of the area in 2017 and 17% in 2018). Moreover, from 2022 to 2024, flooding extended in December, with flooded areas exceeding 21% of the total area. These patterns demonstrate increasingly unpredictable, fragmented, and temporally uneven flood regimes, with some years experiencing exceptionally high flood peaks, followed immediately by years with limited inundation.

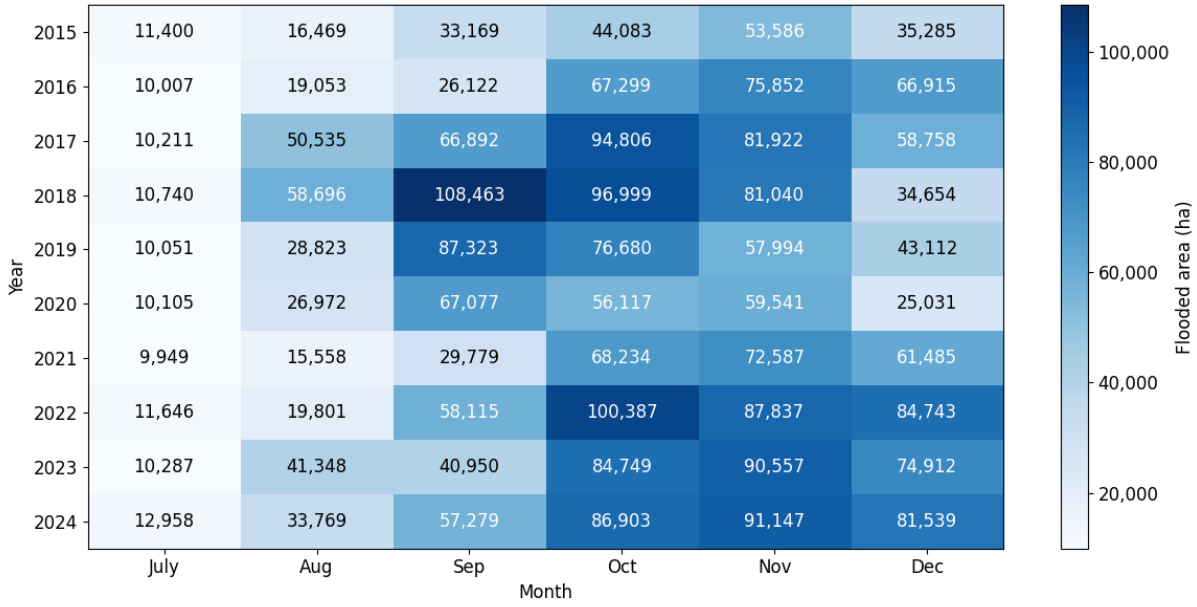

Fig. 4. Monthly flooded area (ha) in An Giang Province from 2015 to 2024 based on Sentinel-1 imagery. The colours indicate flood intensity, with darker shades representing higher inundation levels

4.3 Interannual flood trends and long-term changes

Fig. 5 presents the inter-annual variations in flood extent, showing the mean annual value during the flood season from 2015 to 2024. This analysis aggregates flood extent across the entire flood season of each year to provide the long-term flood dynamics. The figure contrasts years of extreme flooding (e.g., 2017–2018) with years of minimal flooding (e.g., 2015 and 2019–2020), revealing a decadal-scale declining trend. The trend analysis indicates a slight decreasing tendency in the flooded area over time.

From 2016 to 2018, the average annual flood area reached high values, particularly in 2018, with peaks approaching 11% of the area. From 2019 to 2021, the flood area declined markedly, with 2020 reaching the lowest level in the entire series (3% of the area). Despite the declining trend, the period from 2022 to 2024 showed a slight recovery in flood areas, with average levels ranging from 7 to 10%. This reflects that natural flooding has not entirely disappeared, and low-lying inland areas (such as Tri Ton, Chau Phu, and Tinh Bien) continue to serve as flood buffer zones. Overall, the findings indicate that while the flood extent in An Giang is gradually declining, substantial variability remains a key feature of the flood regime.

pISSN 1859-1388
eISSN 2615-9678

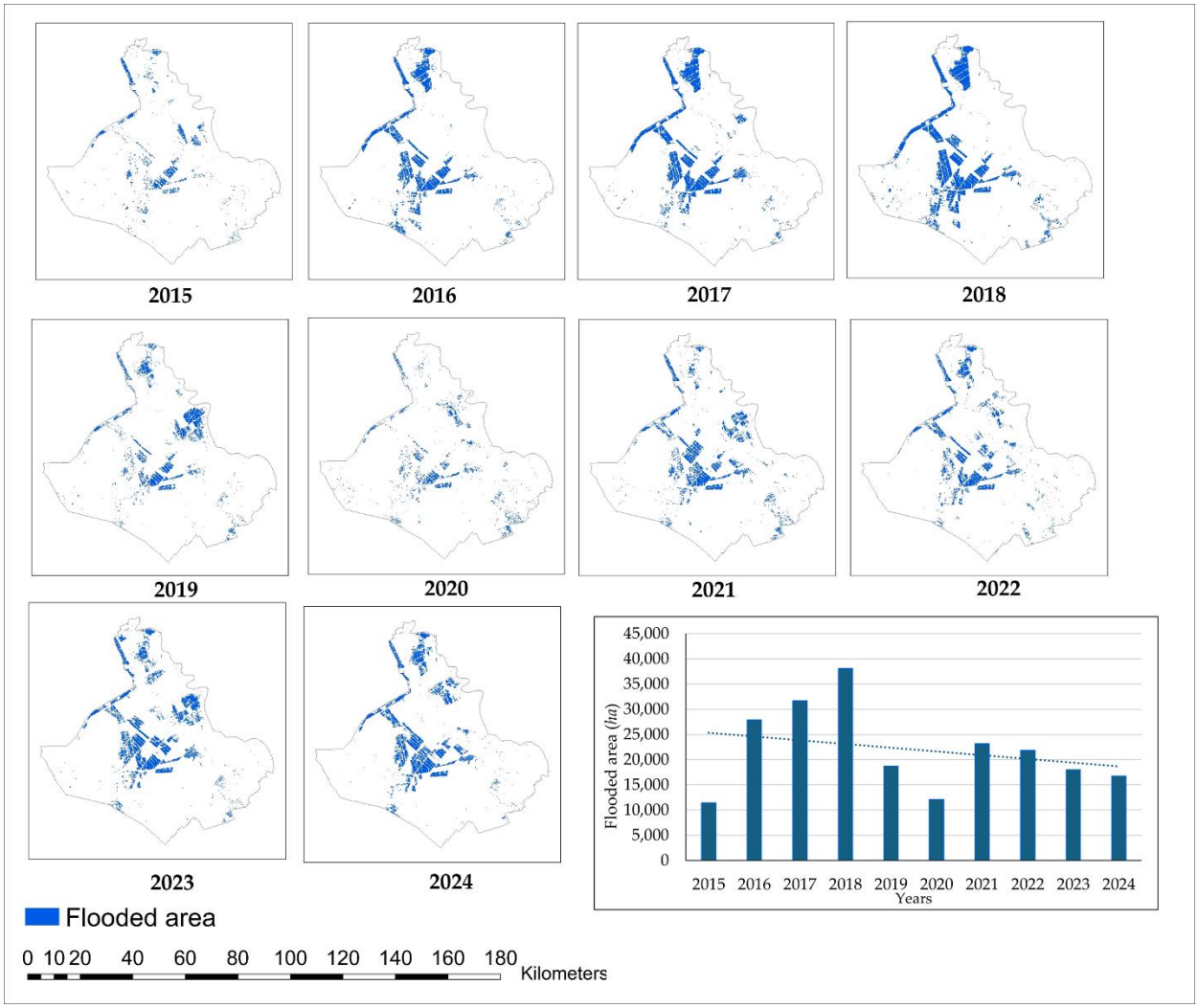

Fig. 5. Interannual flood extent and spatial distribution in An Giang from 2015 to 2024. The trendline shows a slight decreasing tendency in the average flooded area over the study period.

5 Discussion

5.1 Driver of intra-seasonal flood distribution

The intra-seasonal patterns illustrated in Fig. 3 show that floods in An Giang typically start in July, peak in October, and recede by December, with marked contrasts in spatial extent across districts. Low-lying border districts, such as Tri Ton, Tinh Bien, and An Phu, consistently experience early and deep inundation. In contrast, dike-protected areas in Cho Moi, Long Xuyen, and parts of Chau Thanh remain largely unaffected. These spatial differences are consistent with the combined influence of topography and hydraulic infrastructure, particularly rice-based protection dikes.

The expansion of high-dike rings for triple-cropping isolates seasonal floodwaters from protected rice compartments, thereby reducing flooded areas and limiting sediment delivery to rice fields. In contrast, adjacent low-dike or unprotected areas remain flood-prone, with sediment deposition in high-dike fields averaging less than 0.2 kg/m² per year, compared with 1.5–2.0 kg/m² per year in non-dike or low-dike areas [42]. Field sampling across An Giang further documented significant differences in soil properties between high-dike and low-dike

systems, reflecting the geomorphic and agronomic imprint of flood exclusion (soil organic carbon (SOC) content in high-dike fields is 20–40% lower than in low-dike fields) [43]. Beyond soil impacts, sustaining an adequate flood pulse is critical for fish recruitment and functional diversity. Any attenuation or temporal shifts in the flood pulse can depress fisheries and erode ecosystem functions in the lower VMD, particularly in An Giang [44].

Furthermore, the exclusion of floods from high-dike areas may have had broader implications for rice production. Kontgis et al. [45] demonstrated that climate change and reduced seasonal flooding jointly decrease rice productivity in the VMD, underlining the importance of natural flood pulses in maintaining agricultural output. Altogether, these findings emphasise that the spatial distribution of seasonal flooding in An Giang reflects not only natural geomorphological settings but also the ecological and agronomic consequences of extensive dike development.

5.2 Factors controlling interannual flood dynamics

The substantial inter-annual changes—very high floods in 2017–2018 versus minimal floods in 2019–2020—align with an intensifying basin-scale hydropower dams regulation signal. Long-term hydrological analyses have shown that mainstream reservoirs have collectively reduced flood pulses and their frequency at downstream gauges [46], with the influence of dams on the Mekong's flood pulse becoming more pronounced, particularly after 2010 [47]. Meanwhile, sediment trapping upstream has reduced sediment delivery to the VMD by approximately 74%, reinforcing morphological adjustments that, in turn, affect flood hydrodynamics [48].

The ecological and agricultural consequences of this altered flood regime are substantial. Mainstream hydropower dams suppress the amplitude of seasonal pulses, diminish nutrient and sediment replenishment, and disrupt fish recruitment cycles, thereby negatively affecting both fisheries and agriculture in the Lower Mekong Basin [49]. Recent basin-wide assessments further demonstrated that the rapid expansion of dams has fundamentally reshaped river regimes, amplifying extreme droughts and floods, and creating increasingly unpredictable flood timing [50].

Collectively, these findings provide a broader context for the flood patterns observed in An Giang between 2015 and 2024 (Fig. 4). The alternation between exceptionally high and low floods highlights that flood dynamics are no longer solely driven by natural hydrological variability but are increasingly shaped by complex interactions between upstream regulation, sediment reduction, and climate variability. This unpredictability poses significant challenges for water management and agricultural planning in the VMD.

5.3 Long-term flood regime changes and implications

Fig. 5 shows a weak but discernible downward trend in seasonal flood extent over the past ten years from 2015 to 2024. However, in some exceptional years, such as 2017 and 2018, extensive floods still occurred, with flooded areas reaching 11% of the province's total area. Meanwhile, we analysed precipitation data in An Giang from 2015 to 2024, collected from the CHIRPS dataset (a long-term quasi-global gridded product at 0.05° resolution, provided by UCSB/CHG) and accessed via GEE. We found that rainfall over these 10 years experienced a declining trend. Notably, the rainfall in the year with the most significant flood, 2018, was the lowest. This inconsistency between flooding and rainfall indicates that local

pISSN 1859-1388
eISSN 2615-9678

precipitation in An Giang was not necessarily the primary driver of flooding in this area. Instead, the cumulative effects of upstream flow regulation and extensive flood-control works may have modified water-level responses and tidal propagation across the deltaic plain [46, 51]. Notably, the modest recovery since 2022 indicates that natural flooding has not disappeared, but rather is now concentrated in the remaining unprotected lowlands, such as Tri Ton, Chau Phu, and Tinh Bien. These areas serve as natural flood retention zones, storing seasonal floodwaters and sustaining local wetland ecosystems.

Maintaining such flood retention capacity has become a central theme in recent strategies. While high-dike systems have enabled agricultural intensification, they also reduce the spatial extent of natural floods. Modelling studies demonstrated that rice-based protection dikes substantially alter floodwater dynamics and redistribute flooded pressure across the delta [52]. Conversely, ecosystem service assessments highlighted the potential of nature-based flood management strategies to reconcile food production with long-term resilience, ensuring the continued provision of services such as nutrient deposition, groundwater recharge, and biodiversity conservation [53]. These insights underscore that sustaining even limited zones of natural flooding is essential for balancing agricultural and ecological objectives in the VMD.

6 Limitation

This study did not include an independent accuracy assessment of the generated flood maps. Instead, the methodology we applied—Sentinel-1 SAR VH time-series analysis combined with dynamic Otsu thresholding—followed the approach of Tran et al. [13]. Their study developed and tested this approach by deriving water masks from Sentinel-1 and comparing them with Sentinel-2 reference data. Their results demonstrated strong consistency, with coefficients of determination above 0.9 for river environments and around 0.88 for paddy fields, alongside root mean square errors of only 1–4% in water proportion estimates.

By applying this established methodology to An Giang Province, we obtained results that are consistent with the seasonal flood dynamics described in previous studies, which have documented that floods in the Mekong Delta typically peak in the September–October period [48, 54, 55]. Tran et al. [13] demonstrated that the Sentinel-1 Otsu approach achieves high accuracy when validated against Sentinel-2, particularly during the flood peak period from August to November. In our analysis, the most significant flood extents also occurred in this period (e.g., ~31% in 2018 and ~28% in 2022), which supports the reliability of our maps despite the absence of a dedicated accuracy assessment. In our future work, we plan to collect independent ground-truth datasets (e.g., in-situ observations and high-resolution optical classifications) to validate flood extent maps in An Giang directly and further substantiate the accuracy levels of this approach.

7 Conclusions

This study employed Sentinel-1 imagery on the GEE platform to examine flood dynamics in An Giang from 2015 to 2024. The results reveal that while seasonal floods persist, their overall extent has slightly declined over the past ten years, with large year-to-year variability. The most significant floods in An Giang were recorded in 2018 (31% of the area) and 2022 (28%), in contrast to minimal flooding in 2020 (3%), highlighting the unstable nature of the current flood regime. Low-lying areas without-dykes protection, such as Tri Ton, Tinh Bien, and Chau Phu, remained prone to

concentrated flooding and continued to function as key flood retention zones.

These results provide an overview of the unpredictable change in the flood regime, providing a scientific basis to support adaptive water management and land-use planning in An Giang in particular, and in the VMD in general, under the effect of climate change and agricultural activities. In addition, this study demonstrates the effectiveness of Sentinel-1 data on the GEE platform in reliably capturing both seasonal dynamics and long-term changes of flooding.

Acknowledgment

This work was funded by the Asia-Pacific Network for Global Change Research (APN) under project reference number CRRP2023-04MY-Doan Van (Funder ID: doi:10.13039/100005536) and the collaborative research project (Grant number 2023IG-01) of the Disaster Prevention Research Institute of Kyoto University.

References

1. Tran DD, Van Halsema G, Hellegers PJ, Ludwig F, Wyatt A. Questioning triple rice intensification on the Vietnamese Mekong Delta floodplains: An environmental and economic analysis of current land-use trends and alternatives. J Environ Manag. 2018;217:429-441.
2. General Statistics Office of Vietnam. Statistical Yearbook of Vietnam 2021. Hanoi: Statistical Publishing House; 2021.
3. Ministry of Agriculture and Rural Development. Annual Report on Agricultural Production 2022. Hanoi: Agricultural Publishing House; 2022.
4. Tran DD, Van Halsema G, Hellegers PJGJ, Hoang LP, Tran TQ, Kummu M, et al. Assessing impacts of dike construction on the flood dynamics of the Mekong Delta. Hydrol Earth Syst Sci. 2018;22(3):1875-1896.
5. Cochrane TA, Arias ME, Piman T. Historical impact of water infrastructure on water levels of the Mekong River and the Tonle Sap system. Hydrol Earth Syst Sci. 2014;18(11):4529-4541.
6. Dinh TT, Long TX, Nguyen H. Long-Term Assessment of Flood and Drought Phenomena In The Long Xuyen Quadrangle, Vietnamese Mekong Delta. Nativa, 13(1):80-92.
7. Räsänen TA, Lindgren V, Guillaume JHA, Buckley BM, Kummu M. On the spatial and temporal variability of ENSO precipitation and drought teleconnection in mainland Southeast Asia. Clim Past. 2016;12(9):1889-1905.
8. Piman T, Cochrane TA, Arias ME, Green A, Dat ND. Assessment of Flow Changes from Hydropower Development and Operations in Sekong, Sesan, and Srepok Rivers of the Mekong Basin. J Water Resour Plann Manage. 2012;139(6):723-732.
9. Dung NV, Merz B, Bárdossy A, Thang TD, Apel H. Multiobjective automatic calibration of hydrodynamic models utilizing inundation maps and gauge data. Hydrol Earth Syst Sci. 2011;15(4):1339-1354.
10. Nguyen D, Renwick J, McGregor J. Variations of surface temperature and rainfall in Vietnam from 1971 to 2010. Int J Climatol. 2013;34(1):249-264.
11. Chen Y, Huang C, Ticehurst C, Merrin L, Thew P. An evaluation of MODIS daily and 8-day composite products for floodplain and wetland inundation mapping. Wetlands. 2013;33(5):823-835.
12. Torres R, Snoeij P, Geudtner D, Bibby D, Davidson M, Attema E, et al. GMES Sentinel-1 mission. Remote Sens Environ. 2012;120:9-24.
13. Tran KH, Menenti M, Jia L. Surface water mapping and flood monitoring in the Mekong Delta using Sentinel-1 SAR time series and OTSU threshold. Remote Sens. 2022;14(22):5721.
14. Sakamoto T, Van Nguyen N, Kotera A, Ohno H, Ishitsuka N, Yokozawa M. Detecting temporal changes in the extent of annual flooding within the Cambodia and the Vietnamese Mekong Delta from MODIS time-series imagery. Remote Sens Environ. 2007;109(3):295-313.
15. Dang TD, Cochrane TA, Arias ME, Van PDT, De Vries TT. Hydrological alterations from water infrastructure development in the Mekong floodplains. Hydrol Process. 2016; 30(21):3824–3838.
16. Tsyganskaya V, Martinis S, Marzahn P, Ludwig R. Detection of temporary flooded vegetation using Sentinel-1 time series data. Remote Sens. 2018;10(8):1286.

pISSN 1859-1388
eISSN 2615-9678

17. Tiwari V, Kumar V, Matin MA, Thapa A, Ellenburg WL, Gupta N, et al. Flood inundation mapping–Kerala 2018; harnessing the power of SAR, automatic threshold detection method and Google Earth Engine. PLoS One. 2020;15(8):e0237324.

18. Misra A, White K, Nsutezo SF, Straka W, Lavista J. Mapping global floods with 10 years of satellite radar data. Nat Commun. 2025;16(1):60973.

19. Uddin K, Matin MA, Meyer FJ. Operational flood mapping using multi-temporal Sentinel-1 SAR images: a case study from Bangladesh. Remote Sens. 2019;11(13):1581.

20. Lam C, Niculescu S, Bengoufa S. Monitoring and mapping floods and floodable areas in the Mekong Delta (Vietnam) using time-series Sentinel-1 images, convolutional neural network, multi-layer perceptron, and random forest. Remote Sens. 2023;15(8):2001.

21. Hanh LN, Son NH, Lang LPC, Van An N, An TT. Flood mapping and impact assessment in agricultural land in Hoa Vang, Da Nang using remote sensing and Google Earth Engine. VNU J Sci Earth Environ Sci. 2024;40(1):5068.

22. Thao NTP, Linh TT, Ha NTT, Vinh PQ, Linh NT. Mapping flood inundation areas over the lower part of the Con River Basin using Sentinel-1A imagery. Vietnam J Earth Sci. 2020;42(3):15453.

23. Sy HM, Luu C, Bui QD, Ha H, Nguyen DQ. Urban flood risk assessment using Sentinel-1 on the Google Earth Engine: a case study in Thai Nguyen city, Vietnam. Remote Sens Appl Soc Environ. 2023;31:100987.

24. Van Rutten P, Lazaro IB, Muis S, Teklesadik A, Van Den Homberg M. Flood and rice damage mapping for tropical storm Talas in Vietnam using Sentinel-1 SAR data. Remote Sens. 2025;17(13):2171.

25. Nguyen THD, Nguyen TC, Nguyen TNT, Doan TN. Flood inundation mapping using Sentinel-1A in An Giang Province in 2019. Vietnam J Sci Technol. 2020;62(4):36-42.

26. Afifi AS, Magdy A. Flood monitoring in An Giang Province, Vietnam using global flood mapper and Sentinel-1 SAR. Remote Sens Lett. 2024;15(9):883-92.

27. Vanderhoof MK, Alexander L, Christensen J, Solvik K, Nieuwlandt P, Sagehorn M. High-frequency time series comparison of Sentinel-1 and Sentinel-2 satellites for mapping open and vegetated water across the United States (2017–2021). Remote Sens Environ. 2023;288:113498.

28. Van CT, Thuy HTT, Viet C, Anh LN, Van Anh VT, Tran DD. Unveiling flood vulnerability in the Vietnamese Mekong Delta: a case study of An Giang Province. Int J Disaster Risk Reduct. 2024;106:104429.

29. Vu HTD, Tran DD, Schenk A, Nguyen CP, Vu HL, Oberle P, et al. Land use change in the Vietnamese Mekong Delta: new evidence from remote sensing. Sci Total Environ. 2021;813:151918.

30. General Statistics Office of Vietnam. Population and housing census 2019. HanoiL Statistical Publishing House; 2019.

31. Van Khanh Triet N, Dung NV, Fujii H, Kummu M, Merz B, Apel H. Has dyke development in the Vietnamese Mekong Delta shifted flood hazard downstream? Hydrol Earth Syst Sci. 2017;21(8):3991-4010.

32. Ле Т, Нгуен Т, Ку Д, Цветков А, Чыонг Х, Зыонг Ч, Нгуен Д. Meteorological characteristics of the Mekong Delta in the period of 2014–2020. Ecosyst Transform. 2024;7(1):52-69.

33. An Giang Provincial People's Committee. Natural condition [Internet]. 2025 [cited 2025 Jun 1].

34. Minh HVT, Lien BTB, Ngoc DTH, Van Ty T, Ngan NVC, Cong NP, et al. Understanding rainfall distribution characteristics over the Vietnamese Mekong Delta: a comparison between coastal and inland localities. Atmosphere. 2024;15(2):217.

35. Thanh VQ, Roelvink D, Van Der Wegen M, Reyns J, Kernkamp H, Van Vinh G, et al. Flooding in the Mekong Delta: the impact of dyke systems on downstream hydrodynamics. Hydrol Earth Syst Sci. 2020; 24(1):189–212.

36. Dang TD, Cochrane TA, Arias ME, Tri VPD. Future hydrological alterations in the Mekong Delta under the impact of water resources development, land subsidence and sea level rise. J Hydrol Reg Stud. 2018;15:119-33.

37. Mondal A, Le M, Lakshmi V. Land use, climate, and water change in the Vietnamese Mekong Delta (VMD) using earth observation and hydrological modeling. J Hydrol Reg Stud. 2022;42:101132.

38. Vu HTD, Trinh VC, Tran DD, Oberle P, Hinz S, Nestmann F. Evaluating the impacts of rice-based protection dykes on floodwater dynamics in the Vietnamese Mekong Delta using Geographical Impact Factor (GIF). Water. 2021;13(9):1144.

39. Google for Developers. Sentinel-1 SAR GRD: C-band synthetic aperture radar ground range detected, log scaling [Internet]. [cited 2025 Jun 1].

40. Choi H, Jeong J. Speckle noise reduction technique for SAR images using statistical characteristics of speckle noise and discrete wavelet transform. Remote Sens. 2019;11(10):1184.

41. Yommy AS, Liu R, Wu AS. SAR image despeckling using refined Lee filter. In: 2015 7th Int Conf on Intelligent Human–Machine Systems and Cybernetics. Hangzhou, China: IEEE; 2015. p. 260–5.

42. Chapman AD, Darby SE, Hong HM, Tompkins EL, Van TPD. Adaptation and development trade-offs: fluvial sediment deposition and the sustainability of rice-cropping in An Giang Province, Mekong Delta. Clim Change. 2016;137(3–4):593-608.

43. Livsey J, Da CT, Scaini A, Lan THP, Long TX, Berg H, et al. Floods, soil and food – interactions between water management and rice production within An Giang Province, Vietnam. Agric Ecosyst Environ. 2021;320:107589.

44. Wang C, Jiang Z, Zhou L, Dai B, Song Z. A functional group approach reveals important fish recruitments driven by flood pulses in floodplain ecosystem. Ecol Indic. 2018;99:130-9.

45. Kontgis C, Schneider A, Ozdogan M, Kucharik C, Tri VPD, Duc NH, et al. Climate change impacts on rice productivity in the Mekong River Delta. Appl Geogr. 2018;102:71-83.

46. Van Binh D, Kantoush SA, Saber M, Mai NP, Maskey S, Phong DT, et al. Long-term alterations of flow regimes of the Mekong River and adaptation strategies for the Vietnamese Mekong Delta. J Hydrol Reg Stud. 2020;32:100742.

47. Normandin C, Frappart F, Bourrel L, Blarel F, Biancamaria S, Wigneron J, et al. Sharp decline in surface water resources for agriculture and fisheries in the Lower Mekong Basin over 2000–2020. Sci Total Environ. 2024;950:175259.

48. Van Binh D, Kantoush S, Sumi T. Changes to long-term discharge and sediment loads in the Vietnamese Mekong Delta caused by upstream dams. Geomorphology. 2019;353:107011.

49. Yoshida Y, Lee HS, Trung BH, Tran H, Lall MK, Kakar K, et al. Impacts of mainstream hydropower dams on fisheries and agriculture in Lower Mekong Basin. Sustainability. 2020;12(6):2408.

50. Dang H, Pokhrel Y. Evolution of river regimes in the Mekong River Basin over 8 decades and the role of dams in recent hydrological extremes. Hydrol Earth Syst Sci. 2024;28(14):3347-65.

51. Thanh VQ, Roelvink D, Van Der Wegen M, Reyns J, Kernkamp H, Van Vinh G, et al. Flooding in the Mekong Delta: the impact of dyke systems on downstream hydrodynamics. Hydrol Earth Syst Sci. 2020;24(1):189-212.

52. Vu HTD, Trinh VC, Tran DD, Oberle P, Hinz S, Nestmann F. Evaluating the impacts of rice-based protection dykes on floodwater dynamics in the Vietnamese Mekong Delta using Geographical Impact Factor (GIF). Water. 2021;13(9):1144.

53. Dang NA, Benavidez R, Tomscha SA, Nguyen H, Tran DD, Nguyen DTH, et al. Ecosystem service modeling to support nature-based flood water management in the Vietnamese Mekong River Delta. Sustainability. 2021;13(24):13549.

54. Mekong River Commission. State of the Basin Report 2018. Vientiane: MRC Secretariat; 2018.

55. Dinh T, Long TX, Nguyen H. Long-term assessment of flood and drought phenomena in the Long Xuyen Quadrangle, Vietnamese Mekong Delta. Nativa. 2025;13(1):80-92.